

# Applied Stresses and Residual Stresses near the Crack Tip of Precracked Specimens

by Günther Hellwig and Eckard Macherauch  
Institut für Werkstoffkunde I Universität Karlsruhe, Germany

## Abstract

Considering the stress field near the crack tip of a precracked specimen the Williams-Irwin-equations [1] [2] are used. These equations have been derived for the case of an elastically isotropic and infinitely extended plate containing a sharp edge-crack, half as long as the specimen width. In finitely bounded specimens the WI-eq. approximate the real conditions in front of the crack tip if distances are considered which are small, compared with the crack length [3] [4]. In spite of the fundamental importance for fracture mechanics an experimental proof of the WI eq. has not yet been published. The main reason is the difficulty of stress analysis in the area of large stress gradient near the crack tip. The X-ray method of stress analysis seems to be the only successful one in this respect. This paper deals with the measurement of applied and residual stresses in front of the crack tip of precracked steel specimens by means of X-rays.

## Experimental Procedure

Measurements have been performed on unalloyed steel with a carbon content of 0.45 wt-%. After hardening and tempering (6' 820 °C → oil, 2 h 450 °C, 550 °C, 650 °C resp.) the specimens' yield-strengths were  $\sigma_s = 115 \text{ kp/mm}^2$ ,  $83 \text{ kp/mm}^2$ ,  $63 \text{ kp/mm}^2$  resp. . Centercracked specimens without residual stresses have been obtained by fatigue crack generation before heat treatment.

Stresses have been measured perpendicularly to the crack plane, using the X-ray  $\sin^2\psi$ -method [5] ( $\text{CrK}\alpha$ -radiation, {211}-interference-line, back-reflection film system). All stresses are mean values of surface areas with 0.3 mm diameter. Neglecting the influence of elastic anisotropy, for all calculations the mechanical values of Young's modulus ( $E = 21\,000 \text{ kp/mm}^2$ ) and Poisson's ratio ( $\nu = 0.28$ ) have been used.

## Results and Discussion

The stress distributions  $\sigma_y(x)$  in front of a specimen's crack due to three different nominal stresses  $\sigma_n$  are

shown in fig. 1. The specimen ( $2a = 10.5 \text{ mm}$ ,  $\sigma_s = 115 \text{ kp/mm}^2$ ) was free of residual stresses. Using  $\sigma_n = 25 \text{ kp/mm}^2$  (small plastic zone) the maximum stress appears near the crack tip. In the case of  $\sigma_n \geq 35 \text{ kp/mm}^2$  (large plastic zone) the maximum stresses are observed at certain distances ahead the crack tip. These results are typical for all heat-treated steel specimens investigated. As shown in fig. 2, nearly the same stress-distributions in front of the crack are found if specimens with different crack lengths are loaded up to the same K-value. Taking in account the extension of the plastic zone, there is good agreement between the measured and the calculated  $\sigma_y(x)$ -distributions up to  $\sigma_y(x) \approx \sigma_n$ . The drop of stress observed in the plastic zone and the fact  $\sigma_y^{\max}(x) < \sigma_s$ , always fulfilled, may be related to the specific qualities of the X-ray method. It is well established that uniaxially deformed polycrystals show a decrease in the X-ray elastic constants with increasing strain [6]. Therefore, too small stresses will be determined using the bulk elastic properties of the material. Depending on strain discrepancies up to 20 % seems possible. Furthermore, in X-ray stress analysis only surface crystallites will be measured because the X-rays are diffracted only from surface layers. The yield strength of these crystallites seems to be smaller than that of those in the interior of the specimen [7]. This supports  $\sigma_y^{\max}(x) < \sigma_s$ . These results confirm the applicability of the WI-equation in the range  $\omega < x < \frac{a}{2}$  where  $\omega$  is the length of the plastic zone on the ligament. Furthermore, they show that the extension of the plastic zone can be determined approximatively by X-ray stress analysis.

Loading and unloading a precracked specimen originally free of residual stresses  $\sigma_y^R(x)$  should develop residual stresses near the crack tip. Supposing the same notch effect in tension and compression, these residual stresses can be calculated from the superposition of the corresponding stress distributions [8]. In fig. 3 measured and theoretical curves  $\sigma_y^R(x)$  have been compared for a specimen ( $\sigma_s = 63 \text{ kp/mm}^2$ ;  $2a = 12.5 \text{ mm}$ ), unloaded from a nominal stress of  $\sigma_n = 35 \text{ kp/mm}^2$ . Qualitatively, both stress distributions agree well. In both cases  $\sigma_y^{R,\max}(x)$  occur at the end of the plastic zone.

The formation of a fatigue crack causes residual stresses near the crack tip. For example, fig. 4 shows the distribution of residual stresses in front and behind of the crack tip of a heat treated steel specimen ( $\sigma_s = 63 \text{ kp/mm}^2$ ). This specimen was fatigued up to 108 000 cycles with

fluctuating stresses between  $\sigma_{\max} = 40 \text{ kp/mm}^2$  and  $\sigma_{\min} = 9 \text{ kp/mm}^2$ . Thereafter the crack length was 9,5 mm. It is quite apparent from fig. 4 that both, the ligament in front of the crack tip as well as the surface material besides the crack, are under compressive stresses. Obviously, the compensation of the residual stresses is not limited to the uncracked part of the specimen. The changes in the total stress distribution with increasing static load near the tip of the fatigue crack are shown in fig. 4b to 4e.

First of all, the compressive stresses acting on both sides of the crack surface will disappear due to a gradual crack opening. The crack opening stress seems to be about  $10 \text{ kp/mm}^2$ . Up to this stress the effective crack lengths are smaller than the real one and lead to smaller K-values [9] respectively. Nominal stresses  $\sigma_n > 10 \text{ kp/mm}^2$  will yield smaller total stresses near the crack than in the case of specimens free of residual stresses.

References:

- [1] M.L. Williams: J. Appl. Mech., 24, 1957
- [2] G.R. Irwin: J. Appl. Mech., 24, 1957
- [3] H. Küppers: Glastechn. Berichte, 37, 1964/4, p. 185 - 189
- [4] H W. Liu: ASTM STP 381, 1965, 23/26
- [5] E. Macherauch and P. Müller: Z.f. angew. Physik, 13, 1961
- [6] R. Prümmer: Dissertation Universität Karlsruhe, 1967
- [7] D. Emtter and E. Macherauch: Arch.f.Eisenhw. 35, 1964, p. 909
- [8] J.R. Rice: ASTM STP 415, 1967
- [9] W. Elber: Materialprüfung 12, 1970, 6, p.189/193

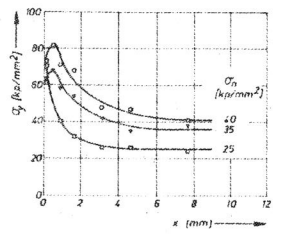


Fig. 1:  $\sigma_y(x)$ -curves at different nominal stresses.  $\sigma_S = 115 \text{ kp/mm}^2$ ,  $2a = 9.5 \text{ mm}$

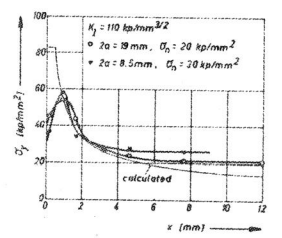


Fig. 2: Measured and calculated  $\sigma_y(x)$ -distributions.  $\sigma_S = 83 \text{ kp/mm}^2$ ;  
 $\circ \sigma_n = 20 \text{ kp/mm}^2$   
 $\nabla \sigma_n = 30 \text{ kp/mm}^2$

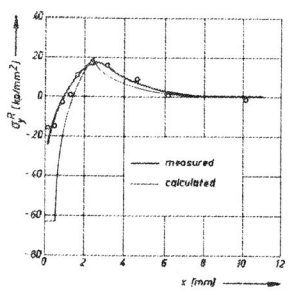


Fig. 3: Measured and calculated  $\sigma_y^R(x)$ -distributions. Unloaded from  $\sigma_n = 35 \text{ kp/mm}^2$ .  $\sigma_S = 63 \text{ kp/mm}^2$ ,  $2a = 12.5 \text{ mm}$ .

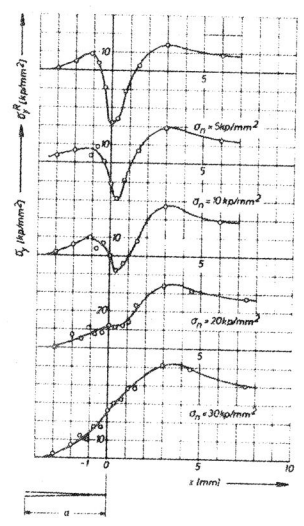


Fig. 4: Residual stresses caused by fatigue crack formation (a). Superposition of residual and applied stresses at different  $\sigma_n$ -values (b) to (e).  $\sigma_S = 63 \text{ kp/mm}^2$ ,  $2a = 9.5 \text{ mm}$ .